

---

# IGCN: INTEGRATIVE GRAPH CONVOLUTIONAL NETWORKS FOR MULTI-MODAL DATA

---

**Cagri Ozdemir**

Department of Computer Science and Engineering  
University of North Texas  
Denton, TX 76205  
cagri.ozdemir@unt.edu

**Mohammad Al Olaimat**

Department of Computer Science and Engineering  
University of North Texas  
Denton, TX 76205  
mohammad.alolaimat@my.unt.edu

**Yashu Vashishath**

Department of Computer Science and Engineering  
University of North Texas  
Denton, TX 76205  
YashuVashishath@my.unt.edu

**Serdar Bozdag**

Department of Computer Science and Engineering  
University of North Texas  
Denton, TX 76205  
serdar.bozdag@unt.edu

**Alzheimer’s Disease Neuroimaging Initiative**

edrake@bwh.harvard.edu

February 1, 2024

## ABSTRACT

Recent advances in Graph Neural Networks (GNN) have led to a considerable growth in graph data modeling for multi-modal data which contains various types of nodes and edges. Although some integrative prediction solutions have been developed recently for network-structured data, these methods have some restrictions. For a node classification task involving multi-modal data, certain data modalities may perform better when predicting one class, while others might excel in predicting a different class. Thus, to obtain a better learning representation, advanced computational methodologies are required for the integrative analysis of multi-modal data. Moreover, existing integrative tools lack a comprehensive and cohesive understanding of the rationale behind their specific predictions, making them unsuitable for enhancing model interpretability. Addressing these restrictions, we introduce a novel integrative neural network approach for multi-modal data networks, named Integrative Graph Convolutional Networks (IGCN)<sup>1</sup>. IGCN learns node embeddings from multiple topologies and fuses the multiple node embeddings into a weighted form by assigning attention coefficients to the node embeddings. Our proposed attention mechanism helps identify which types of data receive more emphasis for each sample to predict a certain class. Therefore, IGCN has the potential to unravel previously unknown characteristics within different node classification tasks. We benchmarked IGCN on several datasets from different domains, including a multi-omics dataset to predict cancer subtypes and a multi-modal clinical dataset to predict the progression of Alzheimer’s disease. Experimental results show that IGCN outperforms or is on par with the state-of-the-art and baseline methods.

## 1 Introduction

The recent developments in deep learning have boosted research in many areas such as computer vision [1], bioinformatics [2], and natural language processing [3]. However, dealing with graph data imposes significant complications on

---

<sup>1</sup>The source code and documentation is available at <https://github.com/bozdaglab/IGCN>

existing deep learning-based models. Unlike images and text data, graphs are complex data structures without a fixed form, such as social networks [4] and biomedical networks [5]. Graphs can have variable numbers of unordered nodes and nodes can have different numbers of neighbors.

In order to analyze graphs more effectively, Graph Convolutional Networks (GCN) [6] has been introduced as an efficient variant of Graph Neural Networks (GNN). GCN provides an effective convolution operation that aggregates different hops of neighbors. Although GCN gives equal importance to all neighbor nodes while aggregating them, Graph Attention Networks (GAT) [7] learns the importance of each neighbor node through an attention mechanism. The attention mechanism gives more weight to the relevant parts and less weight to the less relevant parts in a convolution operation. This specialty consequently allows the model to make more accurate predictions by focusing on the most important information.

Such GNN-based architectures are mostly applicable to homogeneous networks (i.e., one network with one type of node and edge). However, real-world networks mostly have multi-modal form (i.e., having more than one type of node and edge). Employing GCN or GAT on a given multi-modal network can limit the potential information provided by multiple graph structures. Therefore, it is crucial to utilize multiple graph structures, which already exist for many real-world tasks or are empirically generated by some classical graph construction methods, to further boost the learning performance. Several GNN-based approaches have been introduced as integrative computational tools for multi-modal graphs. Relational Graph Convolutional Networks (RGCN) [8] provides relation-specific transformations, i.e. depending on the type and direction of an edge, for large-scale and multi-modal data. Heterogeneous Graph Attention Network (HAN) [9] generates meta-path-based networks from a multi-modal network. The concept of meta-path can be applied to learn a sequence of relations defined between different objects in a multi-modal graph [10]. After generating meta-paths, HAN takes node-level attention (for each node using its meta-path-based neighborhood) and association-level attention (for each meta-path) into consideration simultaneously. HAN employs a multi-layer perceptron (MLP) module to compute class probabilities rather than taking advantage of graph topologies, which could potentially limit the ability of the model to capture complementary information from graph topologies to make predictions. Furthermore, it has been argued that vanilla GCN and GAT methods could outperform HAN after preparing the network in a more fair way [11]. Apart from HAN, in the context of handling graph heterogeneity, Heterogeneous Graph Transformer (HGT) [12] has been developed to maintain representations dependent on node and edge types.

Developing integrative computational tools has also been of immense importance in cancer molecular biology and precision medicine research. Different genomic data types can be obtained to differentiate subgroups in breast cancer [13], which is currently the most commonly diagnosed cancer worldwide [14]. GNN-based methods have recently been applied to breast cancer subtype prediction problem [15, 16]. However, these models are mostly applicable to a single network, thus, missing the information of multiple data modalities. To address this, multi-omics graph convolutional networks (MOGONET) has been introduced as a supervised multi-omics integration framework to predict breast cancer subtypes, which uses a separate GCN for patient similarity networks based on mRNA expression, DNA methylation, and microRNA (miRNA) expression data types [17]. MOGONET utilizes GCN for omics-specific learning. Comparing with the fully connected neural networks, GCN takes advantage of both the omics features and the correlations among samples described by the similarity networks for better classification performance. Besides directly concatenating the label distribution from each omics data type, MOGONET also utilizes View Correlation Discovery Network (VCDN) to explore the cross-omics correlations at the label space for effective multi-omics integration. Another computational tool named SUPREME, a subtype prediction methodology, integrates multiple types of omics data using GCN [18]. To obtain embeddings, SUPREME concatenates the features from each omics data type in the input space and utilizes them as node attributes on each similarity network.

Even though these existing tools provide effective GCN-based solutions for multi-omics integration, they have some limitations. In the context of breast cancer subtype prediction task, different types of omics data have the potential to reveal unique characteristics at the label space. In other words, some omics types may demonstrate superior performance when predicting one subtype, while others might excel in predicting a different subtype. The importance level of different embeddings obtained from different types of omics data networks tends to change from sample to sample, depending on the ground truth labels. Therefore, directly fusing different types of omics data embeddings without considering the sample level importance of different networks may be liable to make wrong predictions and cause some level of performance degradation. Furthermore, multitudes of existing multi-omics integration tools do not explain how and why their models came to the prediction. In predictive modeling, a crucial trade-off arises: Do we merely desire the prediction, or are we interested in understanding the rationale behind it? [19]. Since each of multi-omics types captures a different part of the underlying biology, understanding the 'why' can contribute to a deeper comprehension of the problem and advance the road toward precision medicine in cancer. Moreover, MOGONET employs a VCDN architecture, whereas SUPREME operates an MLP to determine final label distribution at their last layers. Hence, neither MOGONET nor SUPREME takes advantage of the graph topologies in the last layer to make predictions.

This limitation has the potential to restrict the capability of models to capture complementary information from graph topologies to make predictions.

To address these limitations, in this paper, we introduce a novel supervised integrative graph convolutional networks (IGCN) that operates on multi-modal data structures. In IGCN, a multi-GCN module is initially employed to extract node embeddings from each network. An attention module is then proposed to fuse the multiple node embeddings into a weighted form. Unlike previous studies, the attention mechanism assigns different attention coefficients for each node/sample that helps identify which data modality receives more emphasis to predict a certain class type. This feature makes IGCN interpretable in terms of understanding the rationale behind the prediction. IGCN also utilizes fused node embeddings on multiple similarity networks and takes advantage of multiple graph topologies to determine the final predictions. We presented our experimental results on two biomedical node classification tasks: breast cancer subtype classification task from The Cancer Genome Atlas Breast Invasive Carcinoma Collection (TCGA-BRCA) data (<https://portal.gdc.cancer.gov>), Dementia and Mild Cognitive Impairment (MCI) classification task from Alzheimer's Disease Neuroimaging Initiative (ADNI) data (<https://adni.loni.usc.edu/>). We also showcased the experimental outcomes from three additional real-world multi-modal graphs: movie genre prediction from IMDB data (<https://www.imdb.com>), paper type classification task from ACM data (<http://dl.acm.org>), and author research area classification task from DBLP data (<https://dblp.uni-trier.de>). Our experimental results show that our proposed method outperforms or is on par with the state-of-the-art and baseline methods on these five node classification tasks.

The contributions of the proposed work can be summarized as follows:

- We proposed a novel integrative graph convolutional network called IGCN. IGCN operates on multi-modal graph topologies for node classification or a similar downstream task. We applied IGCN to five node classification problems from different domains, showing that IGCN is broadly applicable to many different node classification problems.
- IGCN utilizes a node-level attention mechanism to integrate node embeddings, leading to a better understanding of the rationale behind the predictions.
- Unlike other state-of-the-art methods in the literature, IGCN takes advantage of graph topologies at the last layer to compute the probabilities of class labels.

## 2 The Proposed Method

IGCN is an integrative computational tool operating on multi-modal graph structures. IGCN employs multi-GCN module on graph networks to obtain the node embeddings. An attention module is then utilized to integrate the multiple node embeddings. In the final layer, IGCN takes advantage of multiple graph topologies to determine the final predictions. Graphical illustration of IGCN is shown in Fig. 1.

To obtain the node embeddings from multi-modal graph, each GCN model in IGCN can be defined as:

$$H_i = \sigma(D_i^{-1/2} A_i D_i^{-1/2} X_i W_i), \quad (1)$$

for  $i = 1, 2, \dots, p$ , where  $p$  is the total number of data modalities and  $X_i \in \mathbb{R}^{m \times d}$  is the feature matrix ( $m$  is the number of nodes and  $d$  is the feature size).  $D_i$  and  $W_i$  are the node degree and the learnable weight matrices, respectively.  $\sigma$  is the activation function. We used a single layer GCN to obtain the node embeddings ( $H_i$ ) for each network layer, however, a multi-layer GCN can be considered as outlined in [6].

In our work, the original adjacency matrix  $\hat{A}_i \in \mathbb{R}^{m \times m}$  was constructed by calculating the cosine similarities between pairs of nodes and edges with cosine similarities larger than a threshold  $\epsilon$  were retained. The adjacency matrix can be defined as:

$$\hat{A}_i = \begin{cases} Ind(s(\mathbf{x}_q, \mathbf{x}_w)), & \text{if } q \neq w \text{ and } s(\mathbf{x}_q, \mathbf{x}_w) \geq \epsilon \\ 0, & \text{otherwise} \end{cases} \quad (2)$$

where  $\mathbf{x}_q$  and  $\mathbf{x}_w$  are the node features of the node  $q$  and  $w$ , respectively.  $s(\mathbf{x}_q, \mathbf{x}_w) = \frac{\mathbf{x}_q \cdot \mathbf{x}_w}{\|\mathbf{x}_q\|_2 \|\mathbf{x}_w\|_2}$  is the cosine similarity.  $Ind(\cdot)$  is an indicator function that maps the input to 1 if the input is greater than or equal to  $\epsilon$ , and to 0 otherwise. As shown in Algorithm 1, the threshold  $\epsilon$  can be determined based on a given parameter  $k$  as:

$$k = \frac{1}{m} \sum_{q,w} Ind(s(\mathbf{x}_q, \mathbf{x}_w)). \quad (3)$$

Representing self connection in the adjacency matrix, we can reform the adjacency matrix as:

$$A_i = \hat{A}_i + I, \quad (4)$$

where  $I$  is a  $m \times m$  identity matrix.

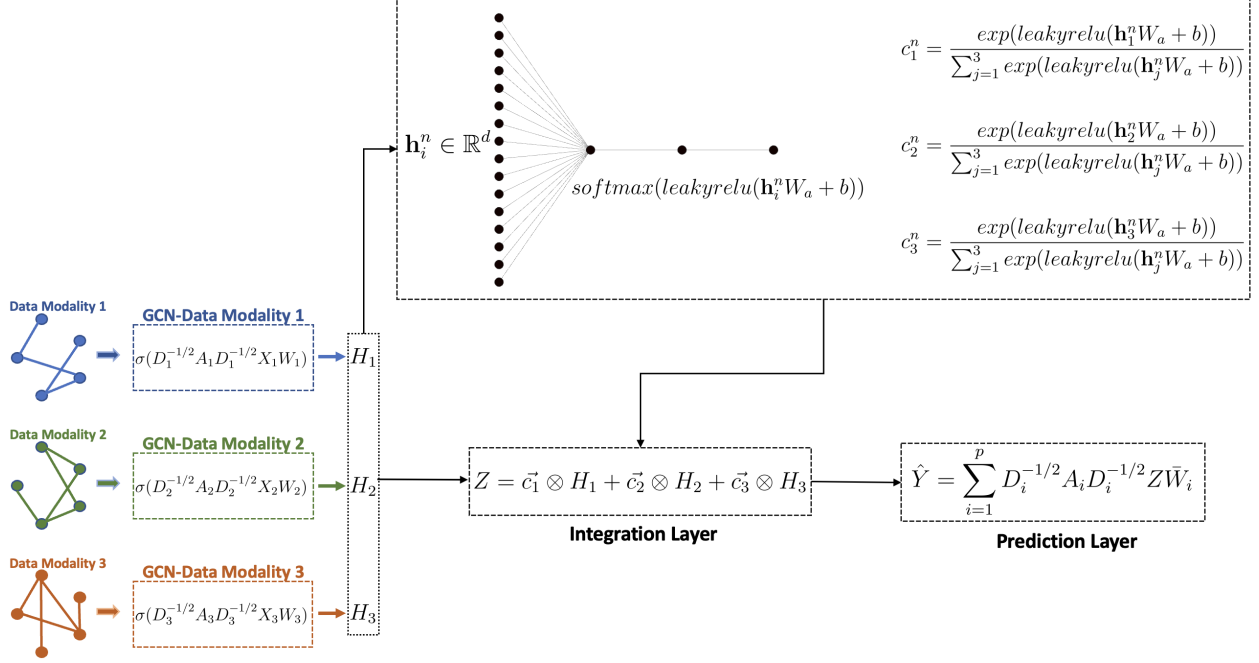


Figure 1: Graphical illustration of IGNC on three similarity networks. IGNC first extracts node embeddings from GCN layers. Then, it employs an integration module to fuse the node embeddings into a weighted form. Finally, a prediction module utilizes fused node embeddings on multiple similarity networks and takes advantage of multiple graph topologies to determine the final predictions.

---

**Algorithm 1** Determine threshold  $\epsilon$  based on pre-specified parameter  $k$

---

**Input:** pre-specified parameter  $k$  and initialize  $\epsilon = 1$   
**Output:**  $\epsilon$   
**while** true **do**  
   $counter = \frac{1}{m} \sum_{q,w} Ind(s(\mathbf{x}_q, \mathbf{x}_w) \geq \epsilon)$   
  **if**  $counter \geq k$  **then**  
    **break**  
  **else**  
     $\epsilon \leftarrow \epsilon - 10^{-6}$   
  **end if**  
**end while**

---

## 2.1 Computing Attention Coefficients and Predictions

After computing node embeddings using Eq. (1), IGNC provides an attention mechanism to fuse multiple node embeddings into a weighted form by assigning attention coefficients to node embeddings. Inspired from [7, 9], attention coefficients can be determined as:

$$c_i^n = \frac{\exp(\text{leakyrelu}(\mathbf{h}_i^n \mathbf{W}_a + b))}{\sum_{j=1}^p \exp(\text{leakyrelu}(\mathbf{h}_j^n \mathbf{W}_a + b))}, \quad (5)$$

where  $\mathbf{h}_i^n \in \mathbb{R}^d$  is the  $n^{th}$  node embedding of the  $i^{th}$  similarity network and  $p$  is the total number of data modalities.  $\mathbf{W}_a \in \mathbb{R}^{d \times 1}$  and  $b \in \mathbb{R}^1$  are learnable weight and bias parameters, respectively. Attention coefficient  $c_i^n \in \mathbb{R}^1$  represents the importance of the  $n^{th}$  node embedding of the  $i^{th}$  network. Attention coefficients can be computed for all nodes of the similarity network and represented as a vector. Therefore, we can fuse the multiple node embeddings using element-wise multiplication, as follows:

$$Z = \sum_{i=1}^p \vec{\mathbf{c}}_i \otimes H_i, \quad (6)$$

where “ $\otimes$ ” denotes element-wise multiplication.  $H_i$  is the node embedding matrix corresponding to  $i^{th}$  similarity network and  $\vec{c}_i$  is the attention coefficient vector for the nodes in the  $i^{th}$  similarity network. It conveys that, although all embeddings are derived from a particular network, individual node embeddings may have distinct coefficient values. For example, consider the vector  $\vec{c}_1$  as a column vector of size  $m$ :

$$\vec{c}_1 = \begin{bmatrix} c_1^1 \\ c_1^2 \\ \vdots \\ c_1^m \end{bmatrix},$$

and let  $H_1$  be a matrix of size  $m \times d$ :

$$H_1 = \begin{bmatrix} h_{1,1} & h_{1,2} & \dots & h_{1,d} \\ h_{2,1} & h_{2,2} & \dots & h_{2,d} \\ \vdots & \vdots & \ddots & \vdots \\ h_{m,1} & h_{m,2} & \dots & h_{m,d} \end{bmatrix}.$$

We also note that  $n^{th}$  row of  $H_1$  can also be represented as a row vector  $\mathbf{h}_1^n$ :

$$\mathbf{h}_1^n = [h_{n,1} \ h_{n,2} \ \dots \ h_{n,d}].$$

The element-wise multiplication of each row of  $\vec{c}_1$  by the corresponding row of  $H_1$  can be represented as follows:

$$\vec{c}_1 \otimes H_1 = \begin{bmatrix} c_1^1 \cdot h_{1,1} & c_1^1 \cdot h_{1,2} & \dots & c_1^1 \cdot h_{1,d} \\ c_1^2 \cdot h_{2,1} & c_1^2 \cdot h_{2,2} & \dots & c_1^2 \cdot h_{2,d} \\ \vdots & \vdots & \ddots & \vdots \\ c_1^m \cdot h_{m,1} & c_1^m \cdot h_{m,2} & \dots & c_1^m \cdot h_{m,d} \end{bmatrix}.$$

IGCN takes advantage of graph topologies to make predictions. In this way, the weighted form of embeddings computed using Eq. (6) is utilized on all similarity networks to obtain the node label predictions. Thus, it can be written as:

$$\hat{Y} = \sum_{i=1}^p D_i^{-1/2} A_i D_i^{-1/2} Z \bar{W}_i. \quad (7)$$

where  $Z$  is computed using Eq. (6) and  $\bar{W}_i$  is a learnable weight matrix corresponding to  $i^{th}$  similarity network.

To determine all learnable weights and biases, we used the cross entropy loss. The lost function can be written as:

$$L_{IGCN} = \sum_{j=1}^m -\log \left( \frac{e^{\langle \hat{\mathbf{y}}_j, \mathbf{y}_j \rangle}}{\sum_k e^{\langle \hat{\mathbf{y}}_j, \mathbf{y}_k \rangle}} \right), \quad (8)$$

where  $\hat{\mathbf{y}}_j \in \mathbb{R}^d$  is the  $j^{th}$  row in  $\hat{Y}$ , which is the predicted label distribution of the  $j^{th}$  training sample.  $\hat{\mathbf{y}}_{j,k}$  is the  $k^{th}$  element in  $\hat{\mathbf{y}}_j$ .  $\mathbf{y}_j \in \mathbb{R}^d$  is the one-hot encoded vector of the ground truth label of the  $j^{th}$  training sample.  $\langle \hat{\mathbf{y}}_j, \mathbf{y}_j \rangle$  represents the inner product of the vector  $\hat{\mathbf{y}}_j$  and the vector  $\mathbf{y}_j$ .

Adam optimization [20] was used as the state-of-the-art for stochastic gradient descent algorithm and 0.5 dropout was added for the first GCN layer. Early stopping was used with the patience of 30 forced to have at least 200 epochs.

### 3 Experiments

In this section, we evaluated the effectiveness of IGCN on TCGA-BRCA, ADNI, IMDB, ACM, and DBLP datasets. The details of the datasets are listed in Table 1. For the multi-modal biomedical integration tasks, we compared the performance of IGCN to the state-of-the-art integrative methods and baseline methods on TCGA-BRCA and ADNI datasets. We also showed the experimental outcomes from three additional real-world multi-modal graphs generated using IMDB, ACM, and DBLP datasets.

#### 3.1 Datasets

**TCGA-BRCA:** Breast tumor samples with mRNA expression, DNA methylation, and miRNA expression data types were collected from TCGA project data portal (available at <https://portal.gdc.cancer.gov>). We used the preprocessed

Dataset	# Node Features	# Samples	# Edges
TCGA-BRCA	mRNA: 1,000 DNA methylation: 1,000 miRNA : 503	Basal-like: 131 HER2-enriched: 46 Luminal A: 436 Luminal B: 147 Normal-like: 115	mRNA: 2,629 DNA methylation: 2,629 miRNA : 2,631
ADNI	cognitive: 12 MRI: 7 SNP: 154	MCI: 272 Dementia: 224	cognitive: 1,490 MRI: 1,490 SNP: 1,490
IMDB	movie: 3,066	action: 1,135 comedy: 1,584 drama: 1,559	MRM: 85,358 MDM: 17,746
ACM	paper: 1,903	database: 1,061 wireless comm.: 1,994 data mining: 970	PAP: 13,879 PLP: 11,889
DBLP	author: 334	database: 1,197 data mining: 745 artificial intel.: 1,109 info retrieval: 1,006	APA: 11,113 APAPA: 40,703 APCPA: 5,000,495 APTPA: 7,043,627

Table 1: Description of the datasets. M: Movie, R: Actor, D: Director, P: Paper, A: Author, L: Field, C: Conference, and T: Term. For TCGA and ADNI, a patient is represented as a node for each layer, but each layer has a different data modality thus the feature size is different, whereas in the other networks, the same feature was used for all the layers, which came from out of bag-based features.

data provided in [17] (available at <https://github.com/txWang/MOGONET>). In the preprocessing of the DNA methylation data, only probes corresponding to the probes in the Illumina Infinium HumanMethylation27 BeadChip were retained. To filter out features with low variance, thresholds 0.1 and 0.001 were applied for mRNA expression and DNA methylation data, respectively. miRNAs with no variation in their expression were filtered out. PAM50 labels of the samples were obtained as the ground truth class labels [13]. Specifically, we have five different class labels: Basal-like, HER2-Enriched, Luminal-A, Luminal-B, and Normal-like. Further details about the preprocessing can be found in [17]. As similarity networks do not naturally exist, three similarity networks were built using Eq. (2) and (3). The quantitative results for TCGA-BRCA dataset shown in Table 2 were generated for the similarity networks, which were built with parameter  $k = 3$  in Eq. (3).

**ADNI:** The ADNI was launched in 2003 as a public-private partnership, led by Principal Investigator Michael W. Weiner, MD. The primary goal of ADNI has been to test whether serial Magnetic Resonance Imaging (MRI), Positron Emission Tomography (PET), other biological markers, and clinical and neuropsychological assessment can be combined to measure the progression of MCI and early Alzheimer’s Disease (AD). Since it was launched, the public-private cooperation has contributed to significant achievements in AD research by sharing data to researchers from all around the world. We employed the ADNImerge R package [21] (available at <https://adni.bitbucket.io/>) to collect longitudinal multi-modal data from all ADNI (<https://adni.loni.usc.edu/>) studies, namely ADNI1, ADNI2, and ADNI-GO. We carried out preprocessing using identical procedures as employed in the PPAD method [22]. In the preprocessing, we have conducted irrelevant feature and visit elimination, addressed missing values through data imputation, and normalized the features. The final dataset consisted of 12 cognitive and 7 MRI features from the most recent visits of the patients. For single nucleotide polymorphism (SNP) data, we used Whole Genome Sequencing (WGS) data of the patients in ADNI dataset. DNA isolation and SNP genotyping process have been described in previous publications [23]. We processed the data using PLINK software package [24]. The following criteria were used for SNP data filtering: missing call rates less than 95% were removed, minor allele frequency (MAF) less than 5% were removed, and Hardy Weinberg equilibrium test of p-value more than  $10^{-6}$  were removed. Samples with call rate less than 95% were filtered. Following the filtration process, we computed the negative logarithm of p-values for the remaining SNPs associated with the phenotypes of patients with MCI and Dementia. Among these SNPs, we identified 154 variants that resulted in p-value smaller than  $5 \times 10^{-8}$ . Finally, we obtained cognitive, MRI, and SNP data for 496 patients with MCI and Dementia ground truth class labels. Since similarity networks do not inherently occur for cognitive, MRI, and SNP data, the similarity networks were built using Eq. (2) and (3). The quantitative results for ADNI dataset shown in Table 2 were generated for the similarity networks, which were built with parameter  $k = 3$  in Eq. (3).

**IMDB:** We collected IMDB data from PyTorch Geometric Library [25], which contains movie (M), actor (R), and director (D) node types. We employed MRM and MDM meta-path-based networks provided by the library. The movies were divided into three classes according to their genre, namely action, comedy, and drama. Movie node features were the elements of a bag-of-words representation, obtained from the library.

**ACM:** We collected ACM data from Deep Graph Library [26]. In this data, there are three node types, namely paper (P), author (A), and field (L). We employed PAP and PLP meta-path-based networks provided by the library. The paper class labels were divided into three classes, namely database, wireless communication, and data mining. Paper node features were the elements of a bag-of-words representation, obtained from the library.

**DBLP:** We collected DBLP data from PyTorch Geometric library [25], which contains paper (P), author (A), conference (C), and term (T) node types. We employed APA, APAPA, APCPA, and APTPA meta-path-based networks provided by the library. The labels of authors correspond to four research areas: database, data mining, artificial intelligence, and information retrieval. Author node features were the elements of a bag-of-words representation, obtained from the library.

### 3.2 Results

We compared IGCN with the state-of-the-art methods (i.e., GCN, GAT, HAN, HGT, RGCN, MOGONET, and SUPREME) as well as baseline methods, namely MLP, Random Forest (RF), and Support Vector Machine (SVM). We evaluated their performance based on four metrics: accuracy, macro F1 score, weighted F1 score, and Matthew's correlation coefficient (MCC).

For TCGA-BRCA and ADNI datasets, we evaluated all the methods on ten different randomly generated training, validation, and test splits. We selected 60% of the samples as the training set, 20% of the samples as the validation set, and 20% of the samples as the test set in a stratified fashion. For each IMDB, ACM, and DBLP datasets, a specific training, validation, and test set is provided by the libraries. Therefore, we repeated each run ten times on these datasets. The validation sets were used across all experiments to tune the hyperparameters (e.g., hidden layer size and learning rate) of the final models. The final models were evaluated on the test data, which was never seen during training and hyperparameter tuning.

Since GCN, GAT, MLP, SVM, and RF are not integrative tools, we evaluated each data modality separately on these methods. For example, we ran GCN on three similarity networks of TCGA-BRCA and ADNI datasets separately and reported the performance by taking the mean of these three results. For each of IMDB, ACM, and DBLP datasets, however, as outlined in [11], we merged all meta-paths by uniting all edges to transform the multi-modal graph into a homogeneous graph, upon which we applied GCN and GAT. We also note that SUPREME can be computed on different combinations of the similarity networks. For each run, we selected the best combination that gives the best macro F1 score on the validation data.

The quantitative results of our comparative experiments are presented in Table 2. The experimental results show that IGCN either achieved the best performance or was on par with the other tools across all metrics and datasets. IGCN outperformed GCN, GAT, MLP, SVM, and RF in TCGA-BRCA, ADNI, IMDB and DBLP datasets showing the importance of multi-modal graph utilization. IGCN achieved the second best performance on ACM dataset. SUPREME achieved slightly better classification performance than IGCN on DBLP dataset. Especially for TCGA-BRCA and ADNI datasets, IGCN surpassed all other integrative and baseline tools with a high difference, highlighting the significance of multi-omics integration. It is also noteworthy that GCN and GAT were run on three similarity networks of TCGA-BRCA dataset (mRNA, DNA methylation, and miRNA networks) and ADNI dataset (cognitive, MRI, SNP networks) separately. The best accuracy was evaluated with GCN on mRNA expression network of TCGA-BRCA dataset, which is  $0.829 \pm 0.016$ . On the other hand, the highest accuracy was attained with GCN on the cognitive measurements network of the ADNI dataset, reaching  $0.856 \pm 0.021$ . These results highlight the importance of multi-data integration because even the top performance achieved is still not superior to that of IGCN. In Fig. 2a and 2b, the boxplots also show the distribution of Matthew's correlation coefficient scores of ten runs on TCGA-BRCA and ADNI datasets. These results indicate that IGCN achieved the best classification performance on both TCGA-BRCA and ADNI datasets.

### 3.3 Attention-driven Interpretability in IGCN

We also investigated which data modalities received high attention on which samples for the node prediction task. Fig. 2c and 2d show the attention coefficients computed for 47 correctly predicted test samples in TCGA-BRCA and ADNI datasets, respectively. For TCGA-BRCA dataset, mRNA expression data had the main contribution toward the prediction of Basal-like, HER2-enriched, Luminal A, and Luminal B breast cancer subtypes, which is expected as PAM50 subtypes are based on mRNA expression data. Interestingly, however, miRNA expression data had the main contribution to predicting Normal-like breast cancer subtype. It is also notable that the attention level of miRNA data is slightly higher in the Luminal A samples compared to the attention level of miRNA data in the Basal-like, HER2-enriched, and Luminal B samples. Concerning to ADNI dataset, the attention coefficients of cognitive data are quite large in the MCI patients, however, there is an interesting attention pattern observed among patients with Dementia.

Dataset	Method	Accuracy	Weighted F1	Macro F1	MCC
TCGA-BRCA	MLP	0.761 $\pm$ 0.012	0.752 $\pm$ 0.015	0.704 $\pm$ 0.022	0.648 $\pm$ 0.020
	SVM	0.774 $\pm$ 0.022	0.771 $\pm$ 0.022	0.736 $\pm$ 0.027	0.668 $\pm$ 0.033
	RF	0.714 $\pm$ 0.020	0.690 $\pm$ 0.023	0.594 $\pm$ 0.036	0.565 $\pm$ 0.032
	GCN	0.787 $\pm$ 0.012	0.782 $\pm$ 0.016	0.743 $\pm$ 0.024	0.685 $\pm$ 0.020
	GAT	0.789 $\pm$ 0.015	0.785 $\pm$ 0.017	0.747 $\pm$ 0.022	0.688 $\pm$ 0.024
	HAN	0.781 $\pm$ 0.025	0.772 $\pm$ 0.036	0.714 $\pm$ 0.069	0.675 $\pm$ 0.039
	HGT	0.795 $\pm$ 0.028	0.789 $\pm$ 0.030	0.739 $\pm$ 0.044	0.697 $\pm$ 0.042
	RGCN	0.825 $\pm$ 0.017	0.824 $\pm$ 0.020	0.791 $\pm$ 0.032	0.744 $\pm$ 0.027
	MOGONET	0.813 $\pm$ 0.013	0.813 $\pm$ 0.014	0.765 $\pm$ 0.027	0.727 $\pm$ 0.019
	SUPREME	0.821 $\pm$ 0.020	0.822 $\pm$ 0.022	0.783 $\pm$ 0.032	0.742 $\pm$ 0.031
ADNI	IGCN	<b>0.858 <math>\pm</math> 0.012</b>	<b>0.861 <math>\pm</math> 0.012</b>	<b>0.831 <math>\pm</math> 0.018</b>	<b>0.795 <math>\pm</math> 0.017</b>
	MLP	0.777 $\pm$ 0.030	0.776 $\pm$ 0.030	0.774 $\pm$ 0.029	0.553 $\pm$ 0.059
	SVM	0.788 $\pm$ 0.030	0.788 $\pm$ 0.030	0.786 $\pm$ 0.030	0.574 $\pm$ 0.060
	RF	0.771 $\pm$ 0.026	0.770 $\pm$ 0.026	0.768 $\pm$ 0.025	0.539 $\pm$ 0.051
	GCN	0.780 $\pm$ 0.026	0.779 $\pm$ 0.026	0.777 $\pm$ 0.026	0.559 $\pm$ 0.053
	GAT	0.772 $\pm$ 0.027	0.772 $\pm$ 0.028	0.777 $\pm$ 0.028	0.545 $\pm$ 0.054
	HAN	0.836 $\pm$ 0.043	0.831 $\pm$ 0.053	0.828 $\pm$ 0.056	0.680 $\pm$ 0.071
	HGT	0.799 $\pm$ 0.058	0.794 $\pm$ 0.066	0.792 $\pm$ 0.069	0.606 $\pm$ 0.112
	RGCN	<u>0.877 <math>\pm</math> 0.024</u>	<u>0.876 <math>\pm</math> 0.024</u>	<u>0.876 <math>\pm</math> 0.024</u>	<u>0.761 <math>\pm</math> 0.040</u>
	MOGONET	0.743 $\pm$ 0.062	0.738 $\pm$ 0.066	0.737 $\pm$ 0.068	0.497 $\pm$ 0.125
IMDB	SUPREME	0.861 $\pm$ 0.036	0.861 $\pm$ 0.036	0.860 $\pm$ 0.037	0.724 $\pm$ 0.075
	IGCN	<b>0.893 <math>\pm</math> 0.028</b>	<b>0.893 <math>\pm</math> 0.028</b>	<b>0.892 <math>\pm</math> 0.028</b>	<b>0.786 <math>\pm</math> 0.054</b>
	MLP	0.492 $\pm$ 0.004	0.489 $\pm$ 0.005	0.492 $\pm$ 0.006	0.230 $\pm$ 0.008
	SVM	0.490 $\pm$ 0.001	0.448 $\pm$ 0.001	0.486 $\pm$ 0.001	0.221 $\pm$ 0.001
	RF	0.487 $\pm$ 0.005	0.479 $\pm$ 0.005	0.474 $\pm$ 0.005	0.214 $\pm$ 0.007
	GCN	0.583 $\pm$ 0.002	<u>0.581 <math>\pm</math> 0.002</u>	<u>0.579 <math>\pm</math> 0.002</u>	0.366 $\pm$ 0.003
	GAT	0.544 $\pm$ 0.006	0.541 $\pm$ 0.007	0.538 $\pm$ 0.007	0.306 $\pm$ 0.010
	HAN	0.573 $\pm$ 0.004	0.569 $\pm$ 0.005	0.567 $\pm$ 0.005	0.352 $\pm$ 0.005
	HGT	0.575 $\pm$ 0.005	0.571 $\pm$ 0.006	0.568 $\pm$ 0.006	0.355 $\pm$ 0.007
	RGCN	0.577 $\pm$ 0.005	0.570 $\pm$ 0.007	0.569 $\pm$ 0.006	0.360 $\pm$ 0.004
ACM	MOGONET	0.492 $\pm$ 0.015	0.493 $\pm$ 0.015	0.491 $\pm$ 0.015	0.241 $\pm$ 0.018
	SUPREME	0.583 $\pm$ 0.005	0.576 $\pm$ 0.007	0.573 $\pm$ 0.008	<u>0.368 <math>\pm</math> 0.007</u>
	IGCN	<b>0.587 <math>\pm</math> 0.002</b>	<b>0.583 <math>\pm</math> 0.002</b>	<b>0.581 <math>\pm</math> 0.002</b>	<b>0.375 <math>\pm</math> 0.004</b>
	MLP	0.869 $\pm$ 0.003	0.868 $\pm$ 0.003	0.864 $\pm$ 0.003	0.790 $\pm$ 0.004
	SVM	0.868 $\pm$ 0.001	0.867 $\pm$ 0.001	0.863 $\pm$ 0.001	0.788 $\pm$ 0.001
	RF	0.872 $\pm$ 0.002	0.871 $\pm$ 0.002	0.867 $\pm$ 0.002	0.795 $\pm$ 0.003
	GCN	<b>0.915 <math>\pm</math> 0.004</b>	<b>0.914 <math>\pm</math> 0.005</b>	<b>0.914 <math>\pm</math> 0.005</b>	<b>0.864 <math>\pm</math> 0.007</b>
	GAT	0.901 $\pm$ 0.009	0.901 $\pm$ 0.009	0.900 $\pm$ 0.010	0.842 $\pm$ 0.014
	HAN	0.883 $\pm$ 0.004	0.881 $\pm$ 0.005	0.880 $\pm$ 0.005	0.813 $\pm$ 0.006
	HGT	0.889 $\pm$ 0.002	0.888 $\pm$ 0.021	0.886 $\pm$ 0.022	0.822 $\pm$ 0.032
DBLP	RGCN	0.906 $\pm$ 0.001	0.904 $\pm$ 0.001	0.904 $\pm$ 0.001	0.849 $\pm$ 0.001
	MOGONET	0.841 $\pm$ 0.030	0.840 $\pm$ 0.031	0.825 $\pm$ 0.040	0.744 $\pm$ 0.048
	SUPREME	0.907 $\pm$ 0.001	0.908 $\pm$ 0.001	0.907 $\pm$ 0.001	0.854 $\pm$ 0.001
	IGCN	0.910 $\pm$ 0.002	0.910 $\pm$ 0.002	0.910 $\pm$ 0.002	0.855 $\pm$ 0.004
	MLP	0.760 $\pm$ 0.004	0.758 $\pm$ 0.004	0.750 $\pm$ 0.004	<b>0.676 <math>\pm</math> 0.005</b>
	SVM	0.753 $\pm$ 0.001	0.752 $\pm$ 0.001	0.742 $\pm$ 0.001	0.669 $\pm$ 0.001
	RF	0.742 $\pm$ 0.002	0.738 $\pm$ 0.002	0.731 $\pm$ 0.002	0.655 $\pm$ 0.002
	GCN	0.807 $\pm$ 0.001	0.806 $\pm$ 0.001	0.797 $\pm$ 0.001	0.740 $\pm$ 0.001
	GAT	0.786 $\pm$ 0.017	0.785 $\pm$ 0.017	0.774 $\pm$ 0.017	0.712 $\pm$ 0.022
	HAN	0.909 $\pm$ 0.001	0.908 $\pm$ 0.001	0.901 $\pm$ 0.001	0.877 $\pm$ 0.001

Table 2: Classification results on TCGA-BRCA, ADNI, IMDB, ACM, and DBLP datasets. The reported values represent the averages along with standard deviations, based on ten runs, for four performance measures, namely: accuracy, macro F1, weighted F1, and Matthew’s correlation coefficient (MCC). The best values for each dataset are shown in bold. The underline is used to signify the second-best performance.

SNP data play a primary role in prediction Dementia for some patients, whereas cognitive features take precedence for others. It is also evident that IGCN fuses different data modalities with a specific ratio for each sample. Existing attention mechanism-based data fusion strategies compute an attention value for each data modality and apply the value on all sample embeddings to integrate different data modalities [9]. However, IGCN finds a golden combination ratio of different data types for each sample. This specialty not only enhances the model’s predictive performance but also captures distinct patterns for various prediction classes, as observed in both TCGA-BRCA dataset (Fig. 2c) and ADNI dataset (Fig. 2d). Since IGCN sheds some light on the interpretability of the effect of different omics data types on a specific class prediction, we strongly believe that our study might pave the way for a new research direction in analyzing different omics data types on different cancer subtype samples for future cancer prediction and prognosis studies.

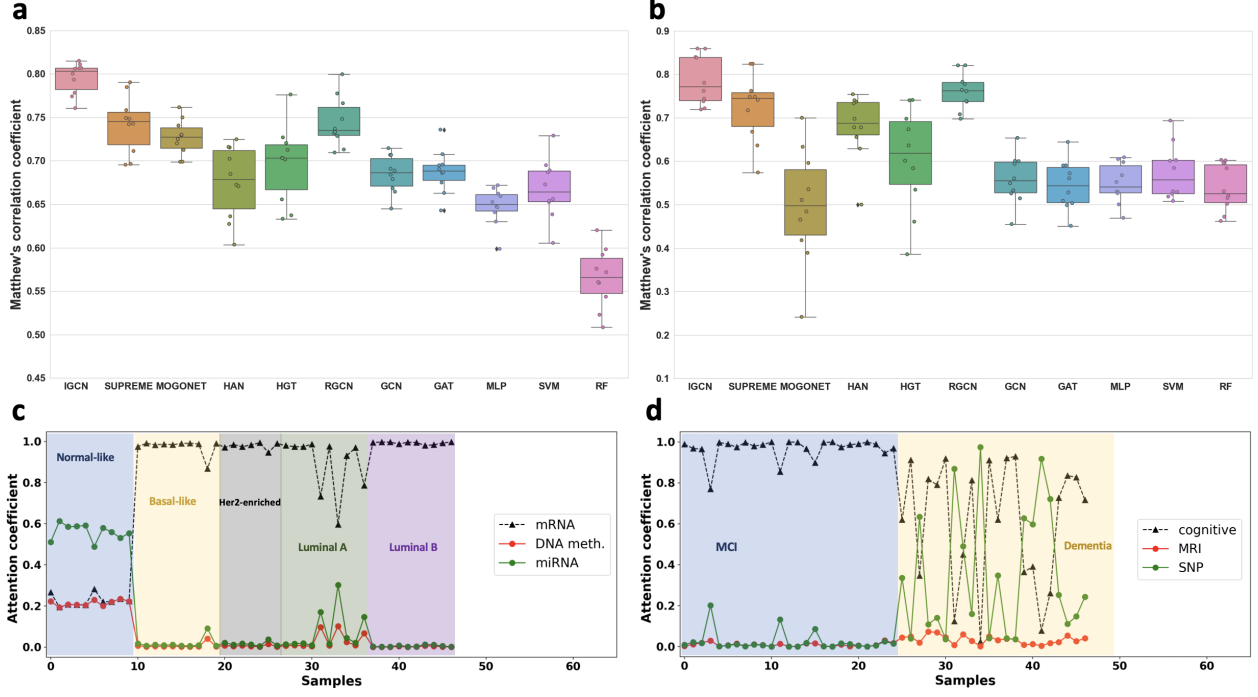


Figure 2: The boxplots show the distribution of Matthew's correlation coefficient scores of ten different runs on (a) TCGA-BRCA and (b) ADNI datasets for all methods. The means and standard deviations of these runs are shown in Table 2. Attention coefficients of 47 test samples of (c) TCGA-BRCA and (d) ADNI datasets. IGCN provides an attention mechanism, which computes a specific attention coefficient for each node embedding. This speciality might allow us to investigate which feature is most informative for each sample in different node type prediction.

### 3.4 Ablation Study

We carried out an ablation study to investigate how the attention mechanism and prediction modules affect the modeling ability of IGCN. Particularly, we developed three variants of IGCN: 1) we disabled the attention mechanism, and computed node embeddings as an average of node embeddings from each network; 2) we disabled the prediction layer (shown in Fig. 1), which utilizes the fused embeddings into the similarity networks, and employed an MLP instead at the final layer to make predictions; and 3) we used the proposed IGCN architecture to observe how disabling of different components affect the model performance. We conducted the experiments on TCGA-BRCA and ADNI datasets and reported the classification performance with macro F1 score measure in Table 3. The results show that both the attention mechanism and the prediction modules are vital in node classification tasks, as the full IGCN setup achieved the best performance.

Components		Macro F1	
Attn. Mech.	Pred.	TCGA-BRCA	ADNI
✗	✓	$0.801 \pm 0.023$	$0.872 \pm 0.025$
✓	✗	$0.816 \pm 0.019$	$0.860 \pm 0.022$
✓	✓	<b><math>0.831 \pm 0.018</math></b>	<b><math>0.892 \pm 0.028</math></b>

Table 3: The average macro F1 scores of different variants of IGCN on TCGA-BRCA and ADNI datasets over ten runs. Attn. Mech.: Attention mechanism, Pred.: Similarity network-based prediction layer.

### 3.5 Performance of IGCN under Different Values of $k$

As similarity networks do not naturally exist for TCGA-BRCA dataset, we built the similarity networks using Eq. (2) and (3). In Eq. (3), the parameter  $k$  represents the average number of edges per node in the similarity network. Choosing a proper  $k$  value depends on the topological structure of the data. In our experiments, the performance of IGCN, SUPREME, MOGONET, RGCN, HGT, and HAN was evaluated on TCGA-BRCA and ADNI datasets for different

similarity networks which were built with  $k = 3, 5, 7$ , and  $9$ . The results shown in Fig. 3 indicate that IGCN was robust to the change of  $k$  value and outperformed other integrative tools under different  $k$  values.

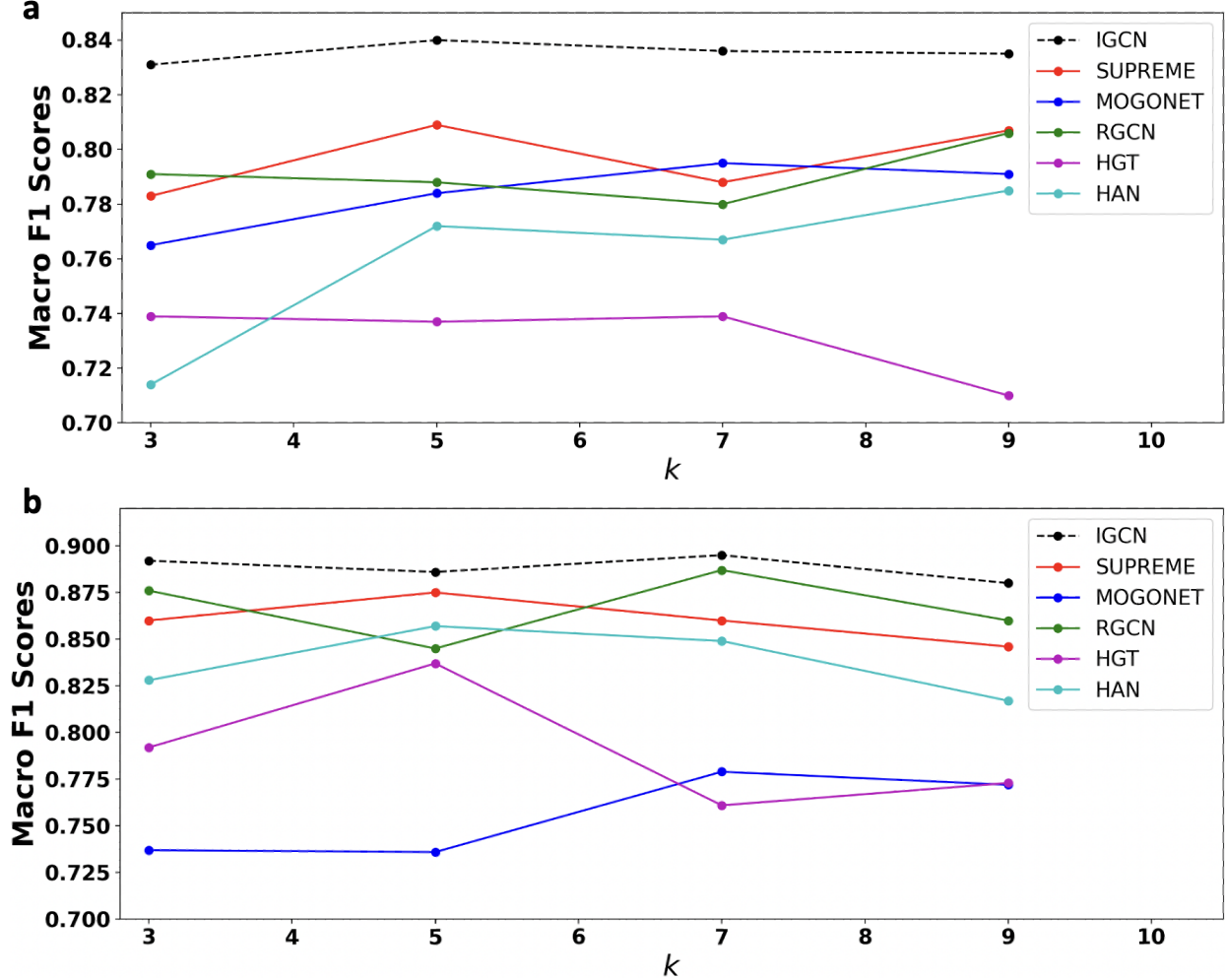


Figure 3: The average macro F1 scores of IGCN, SUPREME, MOGONET, RGCN, HGT, and HAN on (a) TCGA-BRCA and (b) ADNI datasets based on different  $k$  values, which represent the average node degree of the similarity network.

## 4 Conclusion

In this study, we developed a novel integrative neural network architecture that operates on graph-structured multi-modal data. The proposed IGCN integrates multiple network embeddings into a weighted form with attention coefficients that help the identification of which data types are given greater emphasis to predict a specific class type. We demonstrated IGCN's performance using datasets from multiple domains including multi-omics dataset from breast cancer and multi-modal clinical dataset from MCI and Dementia patients. Experimental results illustrate that IGCN outperforms or is on par with the state-of-the-art and baseline methods. Moreover, IGCN is able to interpret its prediction at the test sample level showing which data modality was most effective for the prediction of that sample. Therefore, IGCN has the potential to pave the way for a new research direction in analyzing different omics data types on different cancer subtype samples for future cancer prediction and prognosis studies.

## 5 Acknowledgements

This work was supported by the National Institute of General Medical Sciences of the National Institutes of Health under Award Number R35GM133657. Data collection and sharing for this project was funded by ADNI (National Institutes of Health Grant U01 AG024904) and DOD ADNI (Department of Defense award number W81XWH-12-2-0012). ADNI is funded by the National Institute on Aging, the National Institute of Biomedical Imaging and Bioengineering, and through generous contributions from the following: AbbVie, Alzheimer's Association; Alzheimer's Drug Discovery Foundation; Araclon Biotech; BioClinica, Inc.; Biogen; Bristol-Myers Squibb Company; CereSpir, Inc.; Cogstate; Eisai Inc.; Elan Pharmaceuticals, Inc.; Eli Lilly and Company; EuroImmun; F. Hoffmann-La Roche Ltd and its affiliated company Genentech, Inc.; Fujirebio; GE Healthcare; IXICO Ltd.; Janssen Alzheimer Immunotherapy Research & Development, LLC.; Johnson & Johnson Pharmaceutical Research & Development LLC.; Lumosity; Lundbeck; Merck & Co., Inc.; Meso Scale Diagnostics, LLC.; NeuroRx Research; Neurotrack Technologies; Novartis Pharmaceuticals Corporation; Pfizer Inc.; Piramal Imaging; Servier; Takeda Pharmaceutical Company; and Transition Therapeutics. The Canadian Institutes of Health Research is providing funds to support ADNI clinical sites in Canada. Private sector contributions are facilitated by the Foundation for the National Institutes of Health (www.fnih.org). The grantee organization is the Northern California Institute for Research and Education, and the study is coordinated by the Alzheimer's Therapeutic Research Institute at the University of Southern California. ADNI data are disseminated by the Laboratory for Neuro Imaging at the University of Southern California.

## References

- [1] Alex Krizhevsky, Ilya Sutskever, and Geoffrey E Hinton. Imagenet classification with deep convolutional neural networks. *Advances in neural information processing systems*, 25, 2012.
- [2] Seonwoo Min, Byunghan Lee, and Sungroh Yoon. Deep learning in bioinformatics. *Briefings in bioinformatics*, 18(5):851–869, 2017.
- [3] Tom Young, Devamanyu Hazarika, Soujanya Poria, and Erik Cambria. Recent trends in deep learning based natural language processing. *ieee Computational intelligence magazine*, 13(3):55–75, 2018.
- [4] Etienne Gael Tajeuna, Mohamed Bouguessa, and Shengrui Wang. Modeling and predicting community structure changes in time-evolving social networks. *IEEE Transactions on Knowledge and Data Engineering*, 31(6):1166–1180, 2018.
- [5] Xiang Yue, Zhen Wang, Jingong Huang, Srinivasan Parthasarathy, Soheil Moosavinasab, Yungui Huang, Simon M Lin, Wen Zhang, Ping Zhang, and Huan Sun. Graph embedding on biomedical networks: methods, applications and evaluations. *Bioinformatics*, 36(4):1241–1251, 2020.
- [6] Thomas N Kipf and Max Welling. Semi-supervised classification with graph convolutional networks. *arXiv preprint arXiv:1609.02907*, 2016.
- [7] Petar Veličković, Guillem Cucurull, Arantxa Casanova, Adriana Romero, Pietro Lio, and Yoshua Bengio. Graph attention networks. *arXiv preprint arXiv:1710.10903*, 2017.
- [8] Michael Schlichtkrull, Thomas N Kipf, Peter Bloem, Rianne Van Den Berg, Ivan Titov, and Max Welling. Modeling relational data with graph convolutional networks. In *The Semantic Web: 15th International Conference, ESWC 2018, Heraklion, Crete, Greece, June 3–7, 2018, Proceedings 15*, pages 593–607. Springer, 2018.
- [9] Xiao Wang, Houye Ji, Chuan Shi, Bai Wang, Yanfang Ye, Peng Cui, and Philip S Yu. Heterogeneous graph attention network. In *The world wide web conference*, pages 2022–2032, 2019.
- [10] Yizhou Sun, Jiawei Han, Xifeng Yan, Philip S Yu, and Tianyi Wu. Pathsim: Meta path-based top-k similarity search in heterogeneous information networks. *Proceedings of the VLDB Endowment*, 4(11):992–1003, 2011.
- [11] Qingsong Lv, Ming Ding, Qiang Liu, Yuxiang Chen, Wenzheng Feng, Siming He, Chang Zhou, Jianguo Jiang, Yuxiao Dong, and Jie Tang. Are we really making much progress? revisiting, benchmarking and refining heterogeneous graph neural networks. In *Proceedings of the 27th ACM SIGKDD conference on knowledge discovery & data mining*, pages 1150–1160, 2021.
- [12] Ziniu Hu, Yuxiao Dong, Kuansan Wang, and Yizhou Sun. Heterogeneous graph transformer. In *Proceedings of the web conference 2020*, pages 2704–2710, 2020.
- [13] Joel S Parker, Michael Mullins, Maggie CU Cheang, Samuel Leung, David Voduc, Tammi Vickery, Sherri Davies, Christiane Fauron, Xiaping He, Zhiyuan Hu, et al. Supervised risk predictor of breast cancer based on intrinsic subtypes. *Journal of clinical oncology*, 27(8):1160, 2009.
- [14] J Ferlay, M Ervik, F Lam, M Colombet, L Mery, M Piñeros, A Znaor, I Soerjomataram, and F Bray. Global cancer observatory: cancer today. Lyon, France: International agency for research on cancer, 2018.

- [15] Sungmin Rhee, Seokjun Seo, and Sun Kim. Hybrid approach of relation network and localized graph convolutional filtering for breast cancer subtype classification. *arXiv preprint arXiv:1711.05859*, 2017.
- [16] Ricardo Ramirez, Yu-Chiao Chiu, Allen Herrera, Milad Mostavi, Joshua Ramirez, Yidong Chen, Yufei Huang, and Yu-Fang Jin. Classification of cancer types using graph convolutional neural networks. *Frontiers in physics*, 8:203, 2020.
- [17] Tongxin Wang, Wei Shao, Zhi Huang, Haixu Tang, Jie Zhang, Zhengming Ding, and Kun Huang. Mogonet integrates multi-omics data using graph convolutional networks allowing patient classification and biomarker identification. *Nature Communications*, 12(1):3445, 2021.
- [18] Ziynet Nesibe Kesimoglu and Serdar Bozdag. SUPREME: multiomics data integration using graph convolutional networks. *NAR Genomics and Bioinformatics*, 5(2):lqad063, 2023.
- [19] Finale Doshi-Velez and Been Kim. Towards a rigorous science of interpretable machine learning. *arXiv preprint arXiv:1702.08608*, 2017.
- [20] Diederik P Kingma and Jimmy Ba. Adam: A method for stochastic optimization. *arXiv preprint arXiv:1412.6980*, 2014.
- [21] The ADNI team. *ADNIMERGE: Alzheimer's Disease Neuroimaging Initiative*, 2023. R package version 0.0.1.
- [22] Mohammad Al Olaimat, Jared Martinez, Fahad Saeed, Serdar Bozdag, and ADNI. PPAD: a deep learning architecture to predict progression of alzheimer's disease. *Bioinformatics*, 39(Supplement\_1):i149–i157, 2023.
- [23] Li Shen, Sungeun Kim, Shannon L Risacher, Kwangsik Nho, Shanker Swaminathan, John D West, Tatiana Foroud, Nathan Pankratz, Jason H Moore, Chantel D Sloan, et al. Whole genome association study of brain-wide imaging phenotypes for identifying quantitative trait loci in mci and ad: A study of the adni cohort. *Neuroimage*, 53(3):1051–1063, 2010.
- [24] Shaun Purcell, Benjamin Neale, Kathe Todd-Brown, Lori Thomas, Manuel AR Ferreira, David Bender, Julian Maller, Pamela Sklar, Paul IW De Bakker, Mark J Daly, et al. Plink: a tool set for whole-genome association and population-based linkage analyses. *The American journal of human genetics*, 81(3):559–575, 2007.
- [25] Matthias Fey and Jan Eric Lenssen. Fast graph representation learning with pytorch geometric. *arXiv preprint arXiv:1903.02428*, 2019.
- [26] Minjie Wang, Da Zheng, Zihao Ye, Quan Gan, Mufei Li, Xiang Song, Jinjing Zhou, Chao Ma, Lingfan Yu, Yu Gai, et al. Deep graph library: A graph-centric, highly-performant package for graph neural networks. *arXiv preprint arXiv:1909.01315*, 2019.